PRAMANA
— journal of
physics

Vol. 71, No. 5
November 2008
pp. 965–970

Effect of heat treatment on pore structure in nanocrystalline NiO: A small angle neutron scattering study

J BAHADUR[1,*], D SEN[1], S MAZUMDER[1] and S RAMANATHAN[2]
[1]Solid State Physics Division; [2]Materials Science Division, Bhabha Atomic Research Centre, Mumbai 400 085, India
*Corresponding author. E-mail: jbahadur@barc.gov.in

Abstract. Nanocrystalline nickel oxide powders were calcined at 300, 600 and 900°C and pore structure evolution was followed by small angle neutron scattering (SANS). Pore size distributions at two widely separated size ranges have been revealed. Shrinkage of larger-sized pore with reduction in polydispersity has been observed with increasing heat treatment temperature. The pore structures at various heat treatment temperatures do not scale. This has been attributed to the grain boundary diffusion leading to an asymmetric shrinkage of the pores.

Keywords. Nanoceramics; small angle neutron scattering; sintering; NiO.

PACS Nos 61.10; 61.12

1. Introduction

Since the last decade nanomaterials and in particular, nanoceramics have gained tremendous attention in science and technology. In various functional applications like sensors, solid oxide fuel cell or chemical applications like catalysis etc., nanoceramics have been playing an important role. This is due to the better sinterability of the nanoceramics. Important applications of NiO include the preparation of the cathode materials of the alkaline batteries, antiferromagnetic layers and p-type transparent conducting films [1]. The functional properties of NiO *vis-à-vis* its applicability depend on pore morphology, pore–matrix interface and the porosity. Heat treatment is a process that controls porosity and pore morphology in ceramics [2]. The pore-size distribution and the connectivity of the particles evolve with heat treatment temperature and time. In the case of heat treatment, the porosity reduction and pore shrinkage is mainly governed by the path in which the surface energy gets minimized. The sintering mechanisms of the crystalline particles are divided into densifying mechanisms (e.g. grain boundary diffusion) and non-densifying mechanisms (e.g. surface diffusion). The rigid body motion of the particles takes place in the densifying mechanisms. On the other hand, the

non-densifying mechanism gives the shift of centre of mass of particles but no relative motion.

SANS has been found to be a fruitful non-destructive technique to study the mesoscopic structures in porous materials [3–5]. SANS probes density fluctuations in mesoscopic length scale, it can probe the pore structure in a homogeneously distributed matrix. Compared to other complementary techniques like mercury porosimetry, BET etc., to study the pore structure in a porous material, SANS possesses some special advantages, in particular probing the closed pore structures in addition to the open pores.

2. Experiments

The nanocrystalline powder was synthesized by co-precipitation root. The initial powder was calcined at 300°C. The agglomerate size distribution of the virgin powder is estimated using light scattering. The morphology of the virgin powder has also been examined by scanning electron microscope (SEM). The initial calcined powder sample was also heat treated at 600 and 900°C. SANS experiments have been performed using a double crystal-based medium resolution small angle neutron scattering instrument (MSANS) at Guide Tube Laboratory of the Dhruva reactor at Trombay, India [6]. The instrument consists of a non-dispersive (1, −1) setting of (1 1 1) reflections from silicon single crystals with the specimen between the two crystals. The scattered intensities have been recorded as a function of wave vector transfer q ($=4\pi\sin(\theta)/\lambda$, where 2θ is the scattering angle and λ (=0.312 nm) is the incident neutron wavelength). Before the analysis of the data, SANS profiles of the specimens recorded by the instrument were corrected for instrumental resolution after background and transmission corrections. SANS measurements have been carried out for powder samples which were heat treated at 300, 600 and 900°C, respectively.

3. Data analysis and discussion

Estimated cumulative size distribution of the agglomerate powder particles is depicted in figure 1. The median agglomerate size observed from light scattering (LS) is 0.9 μm. The SEM micrograph is shown in figure 2. It shows the agglomerated nature of the powder. The average agglomerate size observed from SEM picture lies in the range of the size obtained by LS. It is also observed from SEM that on an average there exist two size ranges pores in the specimens. Firstly, pores having larger length scales (Type-1) and other having smaller length scale (Type-2). It is discernible from figure 3 that the whole SANS profile can be divided into two regions and the nature of the two regions gets modified with heat treatment. This feature of the SANS data indicates the presence of two size ranges of the pores in the system.

For simplicity and also to reduce the number of unknown parameters during non-linear least square fitting of the model to the SANS data, the shapes of both Type-1 and Type-2 pores have been assumed as spherical for the present case. In

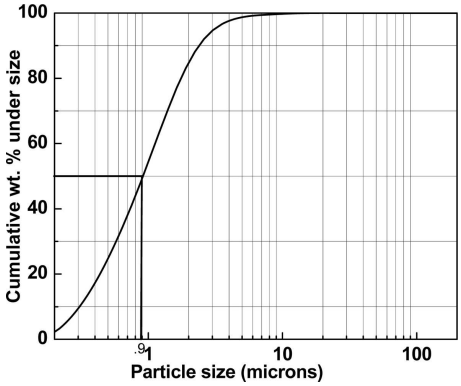

Figure 1. Cumulative agglomerate particle size distribution of the initial NiO powder by light scattering.

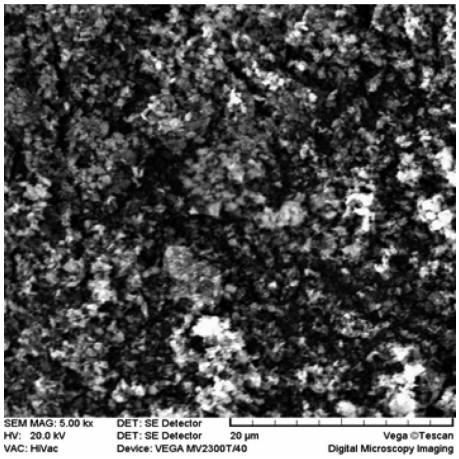

Figure 2. SEM micrograph of the initial virgin powder.

fact this approximation is quite valid for the present case as no structural feature with high aspect ratio is observed from the SEM. The experimental data has been fitted to the following model:

$$I(q) = C_1 \int P(q, R_1) V_{\mathrm{P}}^2 D_{\mathrm{larger}}(R_1) \mathrm{d}R_1 + C_2 \int P(q, R_2) V_{\mathrm{P}}^2 D_{\mathrm{smaller}}(R_2) \mathrm{d}R_2.$$

$D(R)$ has been taken as Weibull distribution as it may be skewed on both sides. The ratio of the number density for the two types of pores can be determined by taking the ratio of C_1 and C_2. The larger length scale pore size distribution for the samples with heat treatment 300, 600 and 900°C, respectively, estimated from the SANS analysis are shown in figure 4. We are interested to see the qualitative features

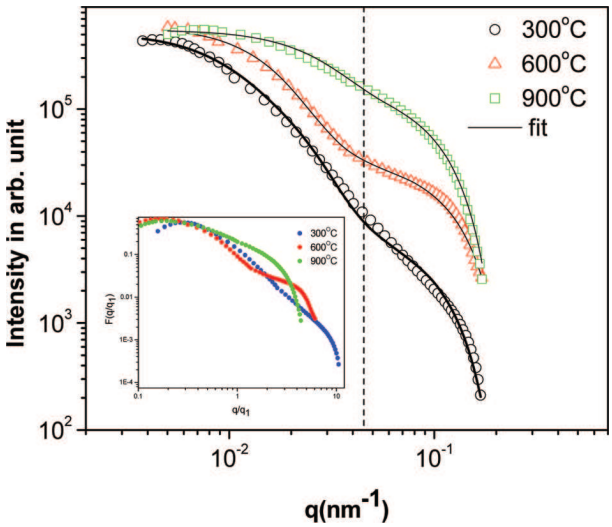

Figure 3. SANS profiles with fitted data. In the inset, the scaled structure factors are plotted with q/q_1.

of the pore size distribution such as polydispersity and the average radius. It is noted that pore size distributions for Type-1 and Type-2 pores are not normalized. It is evident that the polydispersity of the larger length size distribution decreases with increase in heat treatment temperature. Furthermore, the average value of the distribution shifts towards lower radius side. These observations can be explained on the basis of the morphological modification during heat treatment. Neck begins to form between the two adjacent particles during heat treatment. Neck formation is driven by the energy gradient resulting from the difference in curvatures of particle and neck. Densification and grain growth commence in this process. Bulk transport mechanisms primarily, grain boundary diffusion and volume diffusion dominate the heat treatment process. This leads to the shrinkage of the Type-1 pores and also this process involves the reduction in the polydispersity of the pore size. Figure 4 (inset) shows the Type-2 (smaller length scale) pore size distribution for the samples heat treated at 300, 600 and 900°C, respectively.

From figure 4 it is discernible that the distribution for the Type-2 pores lies significantly in the lower size range than that for the Type-1 pores and is much less polydisperse in nature.

To examine the structure evolution function with heat treatment temperature in the light of scaling phenomena, the normalized scaling function $F(q/q_1)$ is given by [7]

$$F\left(\frac{q}{q_1}\right) = \frac{[q_1]^3 I(q)}{\sum_i q_i^2 I(q_i)\delta q_i}, \tag{6}$$

where q_1 and δq_i are the first moment of q and experimental q increment respectively. It is found from the inset of figure 4 that the scaled structure factors do not overlap with each other showing the non-scaling of the structures. The scaling

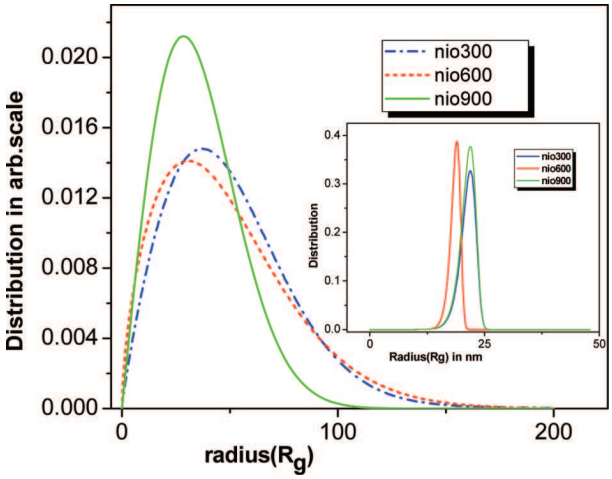

Figure 4. The larger length scale pore size distribution. Inset shows the smaller length scale pore size distribution.

observation has been made to probe the mass diffusion process which is responsible for densification of the nanocrystalline material during heat treatment. If this diffusion process is isotropic during the heat treatment, it is expected that the scaling should hold for the structure factors. In the crystalline solids the primary densification mechanism is the grain boundary diffusion. The surface diffusion is a non-densification mechanism and does not affect significantly the density of the solids but mainly change the surface topology. It is also important to note that the earlier simulation studies on heat treatment behaviour of the amorphous nanoclusters and nanocrystals [8] show that the neck formation is asymmetric for nanocrystals. However, observations showed [8] the breaking of the scaling of the structure factors during heat treatment. In the present case non-scaling of the structure factors *vis-à-vis* the non-scaling of the pore structure is attributed to the above-mentioned asymmetric grain boundary diffusion mechanism. The diffusion process may also be estimated by calculating activation energy. For volume diffusion and grain boundary diffusion the activation energy is different.

4. Conclusions

SANS reveals the existence of pore size distributions in two well-separated size ranges. Shrinkage of the pores occurs with increase in sintering temperature because of the diffusion-based mass transport (primarily, grain boundary diffusion as revealed by the absence of scaling of SANS profiles) of materials in order to minimize surface energy. The pore structures evolve asymmetrically with increasing heat treatment temperature due to the grain boundary diffusion-based mass transport. It may also be confirmed by calculation of activation energy.

References

[1] B Pejova, T Kocareva, M Najdoski and I Grzdanov, *Appl. Surf. Sci.* **165**, 271 (2000)
[2] W D Kingery, H K Bowden and D R Uhlmann, *Introduction to ceramics*, second ed., Wiley Series on the Science and Technology of the Materials (John Wiley & Sons, New York, 1976) p. 1032
[3] D Sen, A K Patra, S Mazumder and S Ramanathan, *J. Alloys Compounds* **340**, 236 (2002)
[4] D Sen, T Mahata, A K Patra, S Mazumder and B P Sharma, *J. Phys.: Condens. Matter* **16**, 6229 (2004)
[5] S Mazumder, D Sen, S K Roy, M Hainbuchner, M Baron and H Rauch, *J. Phys.: Condens. Matter* **13**, 5089 (2001)
[6] S Mazumder, D Sen, T Sarvanan and P R Vijayraghavan, *J. Neutron Res.* **9**, 39 (2001)
[7] S Mazumder, D Sen, I S Batra, R Tewari, G K Dey, S Banerjee, A Sequeira, H Amentisch and S Bernstorff, *Phys. Rev.* **B60**, 822 (1999)
[8] K Tsuruta, A Omeltchenko, R K Kalia and P Vashishta, *Europhys. Lett.* **33(6)**, 441 (1996)